I&EC research
Industrial & Engineering Chemistry Research

Article

pubs.acs.org/IECR

Simple and Efficient Procedure for the Synthesis of Ferrogels Based on Physically Cross-Linked PVA

Jimena S. Gonzalez,*[,†] Cristina E. Hoppe,[†] Pedro Mendoza Zélis,[‡] Lorena Arciniegas,[‡] Gustavo A. Pasquevich,[‡] Francisco H. Sánchez,[‡] and Vera A. Alvarez[†]

[†]Institute of Materials Science and Technology (INTEMA), University of Mar del Plata and National Research Council (CONICET), Avenida J. B. Justo 4302, 7600 Mar del Plata, Argentina

[‡]Physics Department, Physics Institute of La Plata (IFLP-FCE), University of La Plata and National Research Council (CONICET), CC 67, 1900 La Plata, Argentina

ABSTRACT: Ferrogels with well-dispersed single-domain magnetic nanoparticles (NPs) were obtained by the infusion of iron salts in physically cross-linked poly(vinyl alcohol) (PVA) hydrogels followed by coprecipitation. Freeze−thaw (F−T) cycling was used as a cryogenic technique to form mechanically strong and highly swellable hydrogels. The networked structure of the final material was used as a constrained environment for the precipitation of iron oxide NPs and formation of the magnetic gel. A homogeneous, single-domain ensemble of more than 15 wt % iron oxide NPs (in only one cycle of absorption) could be obtained through this easy technique. Moreover, the capacity of these magnetic ferrogels to absorb high amounts of ethanol/water solutions allows impregnation of these materials with ibuprofen and subsequent release of the drug at physiological pH. The biocompatibility of the components and the use of the nontoxic PVA cross-linking strategy (F−T cycling) make these materials promising for drug-delivery applications.

INTRODUCTION

The rational combination of nanostructures with polymers has proved to be a powerful tool for the development of new stimulus-responsive multifunctional materials.[1] Among polymeric matrixes used in nanocomposites, hydrogels are especially attractive and the ideal choice for potential applications in the biomedical, environmental, and pharmaceutical fields.[2] Hydrogels are networks constituted by cross-linked hydrophilic polymer chains with the capacity of absorbing large amounts of water and biological fluids.[3] In the past several years, the interest and attention paid to hydrogels have progressively changed from large-scale products toward more sophisticated applications requiring improved performance.[2b,c,4] This is the case, for example, for stimulus-responsive hydrogels[4b,c] and biomimetic materials,[4a] with multiple and promising applications in actuation, in vitro diagnostics, tissue engineering, and so on. Ferrogels are a class of stimulus-responsive materials composed of magnetic nanoparticles (NPs) embedded in a gel matrix.[5] The synergic combination of magnetic NPs with the soft, hydrophilic, and wet matrix of hydrogels enables the creation of materials with unique and advanced properties useful for the design of smart drug-delivery systems, actuators, and sensors. For example, the presence of NPs enables the building of materials that can be deformed[5b,c,6] or heated[7] by the action of a magnetic field. In the presence of magnetic forces, because of the elastic character of ferrogels, particle movement couples to gel movement, producing significant deformation and/or changes in porosity under the action of quite moderate magnetic fields.[5b,c] These mechanical actions would be responsible for changes in drug release and bursting, on−off behavior observed for some ferrogel systems.[6,8] On the other hand, the action of an alternating magnetic field produces remote heating of the system through the hyperthermal effect that occurs by Néel (inner fluctuation of the magnetic moment) and Brown (rotation of the whole particle) relaxation mechanisms of single-domain superparamagnetic NPs.[7a] In addition to these relevant magnetic properties, the particular affinity of the NP surface for molecules and/or ions could, in some cases, confer sequestering and/or chelating abilities to the gel. These properties are expected to depend strongly on the ferrogel structure (cross-linking density, NP dispersion level, swelling ability)[9] and on environmental conditions such as pH and ionic force.

The way in which ferrogels are synthesized is an important issue to address regarding their properties and potential applications.[5a] For most biomedical and pharmaceutical applications, the use of nontoxic procedures and biocompatible reagents is an almost unavoidable requirement. Poly(vinyl alcohol) is a very well-known biocompatible hydrophilic polymer that has been widely used for the production of commercial hydrogels[3,10] and has a high potential to become an indispensable tool in the design of biomaterials.[11] In the past several years, the use of this polymer as a matrix for the development of ferrogels has been intensively investigated with relative success.[5a,10] Incorporation of NPs in the matrix has commonly been carried out by two different approaches: incorporation of coated or uncoated preformed NPs in solutions of a linear polymer, followed by chemical or physical cross-linking,[5a,12] or formation of NPs in the presence of the polymer, followed by network formation.[5a,13] An alternative

Received: August 13, 2013
Revised: October 29, 2013
Accepted: November 29, 2013
Published: November 29, 2013

approach based on the simultaneous formation of NPs and cross-linking of poly(vinyl alcohol) (PVA) has recently been reported for the synthesis of ferrogel beads.[14] A less explored strategy is the use of the cross-linked polymer network as a constrained environment for the generation of NPs. Some of the advantages of this procedure are the use of preformed, well-characterized hydrogel samples (formed in the absence of NPs) and the possibility of controlling the NP size by constraints imposed by the cross-linked network. In this procedure, hydrogels are swollen with adequate metal precursors that can be subsequently transformed into NPs through the action of an appropriate chemical reagent.[5a] This approach has recently been used for the incorporation of iron oxide NPs in chemically cross-linked hydrogels[15] and also for the synthesis of magnetic physical organogels.[16] In this work, we use this strategy to synthesize highly loaded, well-dispersed magnetic materials from physically cross-linked PVA hydrogels obtained by freeze−thaw (F−T) cycling, a cryogenic and environmentally friendly technique.[10,17] The high swelling capacity and good mechanical properties of physical PVA hydrogels obtained by F−T cycling[18] make such hydrogels ideal candidates as hosts for the development of ferrogels by infusion. Moreover, the presence of OH functional groups in PVA chains can be very useful for the initial binding of metal Fe^{3+} and Fe^{2+} ions and the subsequent stabilization of formed NPs. The biocompatibility of PVA and the nontoxic procedure used for cross-linking make this approach very useful for the development of new materials with applications in drug release.

MATERIALS AND METHODS

Preparation of Ferrogel Samples. PVA hydrogels were obtained by three cycles of freezing−thawing (F−T) applied to 10 wt % PVA aqueous solutions (93500 g/mol, Sigma-Aldrich). These preformed, cross-linked PVA hydrogel samples (typical sample weight, 50 mg) were immersed in a solution of 12.15 g of iron(III) chloride hexahydrate and 6.07 g of iron(II) sulfate heptahydrate (from Cicarelli Laboratory, San Lorenzo, Argentina) in 100 mL of distilled water and equilibrated for 24 h. The hydrogels loaded with iron(II) and iron(III) ions were removed from the solution, washed with deionized water, placed in a solution of ammonia, and left for 1 h to produce coprecipitation of magnetic nanoparticles inside the gel. The resultant ferrogel was removed, washed, and allowed to dry at room temperature. Hereafter, this material is referred to as the dry ferrogel sample. To study the magnetic properties of the hydrated material, small pieces of ferrogel were encapsulated with excess of water in sealed pieces of thermoshrinkable tube having a capacity of 100 μL. This material is referred to hereafter as the hydrated ferrogel sample.

Physical, Chemical, and Magnetic Characterization of the Samples. Transmission electron microscopy (TEM) images were obtained using a Philips CM-12 microscope operated at an accelerating voltage of 100 kV. Images were obtained from ultrathin sections that were cut with a cryo-ultramicrotome. The average size of the magnetic NP core was determined using several images and employing more than 100 particles/image. Field-emission scanning electron microscopy (FESEM) images were obtained with a Zeiss ULTRA plus instrument. Samples were swollen in distilled water, frozen, lyophilized, and then cryofractured with liquid N_2 before testing.

Differential scanning calorimetry (DSC) measurements were carried out in a TA Q 2000 instrument. Dynamic scans were performed from −40 to 250 °C at 10 °C/min, under a N_2 atmosphere. The melting temperature (T_m) and degree of crystallinity were obtained from the resulting thermograms. Before DSC analysis, gel samples were dried for 48 h at 37 °C. The degree of crystallinity (X_{cr}, %) was calculated as

$$X_{cr}\ (\%) = \frac{\Delta H}{\Delta H^0 W_{PVA}} \times 100\% \quad (1)$$

where ΔH was determined by integrating the area under the melting peak over the range 190−240 °C, ΔH^0 is the theoretical heat required to melt a 100% crystalline PVA sample (138.6 J/g),[19] and W_{PVA} is the weight fraction of PVA in the ferrogel.

Thermogravimetric analysis (TGA) was performed with a Shimadzu TGA-DTGA 50 instrument from room temperature to 900 °C at 10 °C/min under an air atmosphere. The degradation temperature (T_p) and iron oxide content, reported as the weight percentage of the fully oxidized crystalline phase, Fe_2O_3, were obtained from these measurements.

Swelling determinations were carried out in distilled water and in ibuprofen solution at 25 °C. Ibuprofen solution was prepared by mixing 75 mg of the drug (Fluka, 98%) with 2.5 mL of distilled H_2O and 12.5 mL of ethanol under constant stirring for 36 h at 32 °C. All samples were dried before immersion at 37 °C for 48 h. The equilibrium swelling degree (W_∞, %) was determined as

$$W_\infty\ (\%) = \frac{W_f - W_i}{W_i} \times 100\% \quad (2)$$

where W_i is the initial weight of the samples before immersion and W_f is the final weight of the sample at equilibrium water content.

The magnetic properties [measurements of mass magnetization (M) versus magnetic field, of M versus temperature after zero-field cooling (ZFC) and field cooling (FC) from room temperature, and of saturation magnetization (M_S) versus temperature]were performed with a MPMS-XL superconducting quantum interference device (SQUID) from Quantum Design, Inc.

The mass magnetization versus magnetic field measurements were performed up to 2400 kA/m. The ZFC/FC measurement procedure was carried out as follows: First, the sample was cooled from 300 to 5 K in zero magnetic field. Then, a static magnetic field of 50 Oe was applied, and the magnetization was measured as the temperature was increased to 300 K. Finally, the sample was cooled again to 5 K under the same applied magnetic field (50 Oe), and the magnetization was measured as the sample was heated from 5 to 300 K. Curves of M_S versus T were obtained under an applied field of 2000 kA/m.

Ibuprofen Absorption and Release Studies. Dried hydrogel samples were allowed to absorb a 3 mg/mL aqueous/ethanol solution of ibuprofen until reaching maximum swelling degree (approximately 24 h). Aqueous/ethanol (50/50) solutions were used because of the poor solubility of ibuprofen in water.[20] The resulting gels were stored at room temperature for 48 h to eliminate the absorbed water. Then, 50 mg of the loaded gels was placed in 5 mL of phosphate buffer (pH 7.4) at 37 °C. At certain times, aliquots of 600 μL were removed, and the same volume was replaced by fresh buffer. The ibuprofen concentration was recorded by measuring the absorbance in phosphate buffer solution at a wavelength of 264 nm. Buffer solutions were prepared from potassium phosphate

dx.doi.org/10.1021/ie402652j | Ind. Eng. Chem. Res. 2014, 53, 214−221

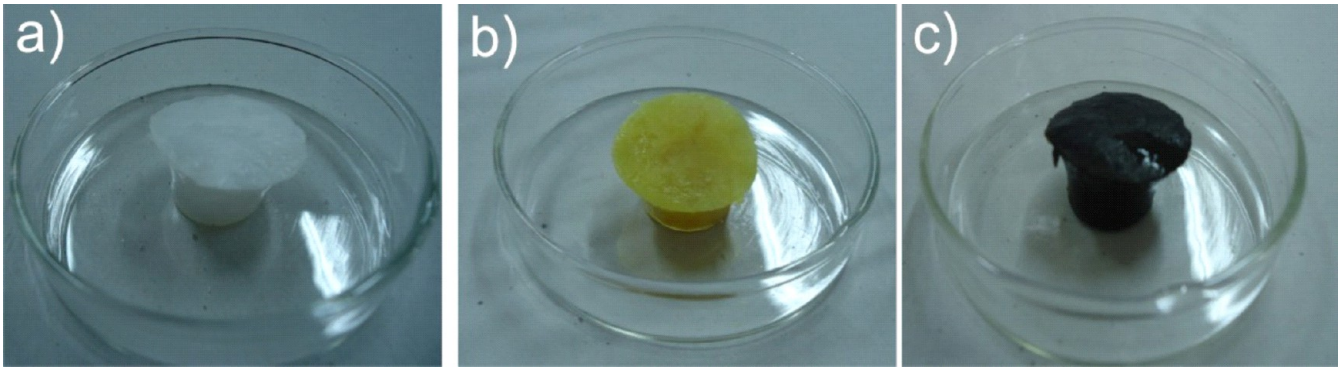

Figure 1. Preparation of ferrogel by infusion of iron salts in a PVA hydrogel and subsequent coprecipitation of magnetic NPs: (a) hydrogel, (b) swollen hydrogel in iron salt solution, (c) ferrogel (after precipitation).

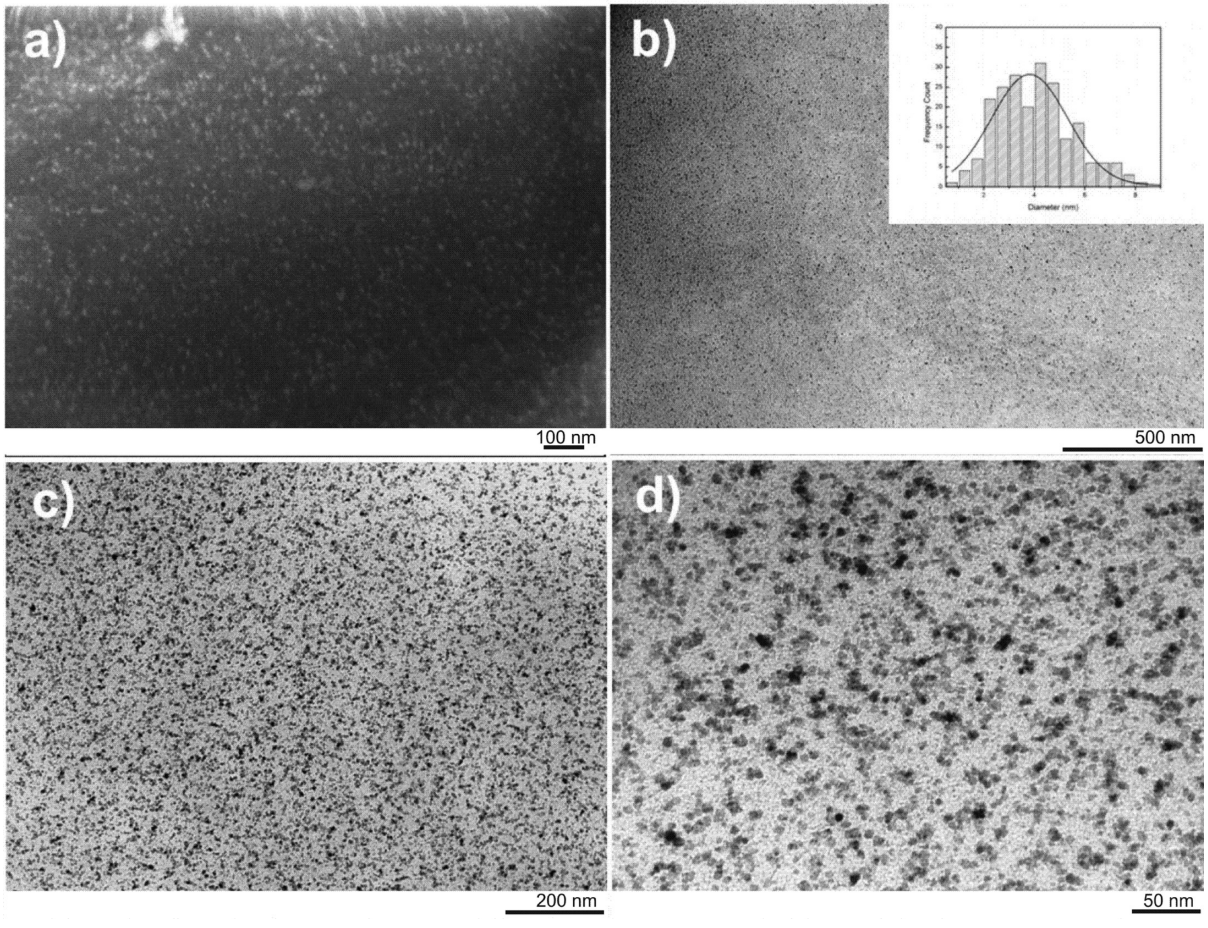

Figure 2. (a) FESEM and (b–d) TEM micrographs of the ferrogel containing 15.7 wt % iron oxide NPs. The inset in panel b shows the size distribution curve for NPs in the matrix.

monobasic anhydrous and sodium phosphate dibasic, both obtained from Sigma-Aldrich, Tokyo, Japan.

RESULTS AND DISCUSSION

Synthesis of Ferrogels. Macroscopic changes observed in the hydrogel during infusion and coprecipitation of NP precursors can be observed in Figure 1. The transparent and colorless PVA hydrogel developed an orange color after the first immersion step as a consequence of infiltration of iron salts. During the final step of the procedure, the samples became dark brown by the action of ammonium hydroxide, indicating the formation of magnetite NPs. TGA measurements revealed that the final iron oxide content was 15.7 wt %. The amount of magnetite formed inside the gel was estimated on the basis of stoichiometric calculations that considered the total concentration of salts in the swollen state to be identical to that of the initial solution. This implies that iron oxide formation is controlled by the degree of swelling (a higher degree of swelling is associated with a higher amount of solution entering the gel and a higher total amount of precursors available for magnetite formation). This is only a rough estimation because fractioning of salts between the swollen gel and the outside solution cannot be discarded. The specific affinity of ions for the PVA structure, for example, could conduct a higher

dx.doi.org/10.1021/ie402652j | Ind. Eng. Chem. Res. 2014, 53, 214–221

concentration of salts inside the gel with respect to the immersion solution. In our case, the maximum swelling degree, attained after 6 h of immersion in the salt solution, was 340%. This value gives a maximum of 11.4 wt % iron salts loaded in the gel [33 wt % Fe(II) salt and 67 wt % Fe(III) salt]. From these values, an iron oxide content as Fe_2O_3 of about 13.3 wt % was obtained. This value is slightly lower than that found by TGA. However, considering the experimental errors associated with the determinations of both the swelling degree and the total inorganic content, the obtained values are still reasonable. As previously discussed, small deviations from this estimation might also be due to an underestimation of the salt loading in the gel, which would indicate a preference by the ions to form complexes with the PVA structure.

TEM images (Figure 2) showed an excellent dispersion of NPs, with a characteristic mean diameter of 4 nm in the PVA matrix. Low size and polydispersity probably arise from physical constraints on NP growth imposed by the matrix during coprecipitation.

The XRD spectra of ferrogel and hydrogel samples are shown in Figure 3. Diffraction peaks located at 19.8° and 22.9° (2θ) (marked with *) were assigned to semicrystalline PVA and correspond to the (101) and ($10\bar{1}$) reflection planes, respectively.[21] The additional peak at 35.5° (2θ) can be assigned to the most intense diffraction peak of magnetite or maghemite and corresponds to the (311) reflection of the crystal struture (JCPDS card no. 19-0629, Joint Committee on Powder Diffraction Standards), confirming the presence of these oxides in the gel.

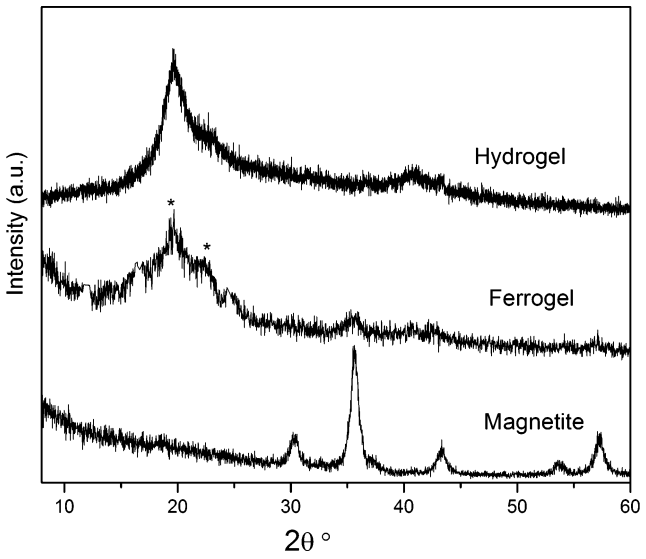

Figure 3. XRD curves obtained for hydrogel, ferrogel, and magnetite samples.

Table 1 displays the thermal results obtained by DSC and TGA. Figure 4 also shows DSC, TGA, and DTG curves for the hydro- and ferrogels. For the described synthesis conditions, TGA measurements revealed an iron content higher than 15 wt %, which indicates that the process is efficient for the inclusion of relatively high amounts of NPs in the hydrogel matrix. For each sample, the peak temperatures of degradation (T_p) were determined from the DTG curves (Figure 4) at the maximum weight loss rate. The degradation temperature of the ferrogel was higher than that of the neat matrix, which is possibly associated with the strong interaction between the matrix and the nanometric phase. These polymer−filler interactions restrict polymer chain mobility and reduce the diffusivity of attacking agents within the polymer matrix, making NPs act as a heating barrier and delaying degradation of the matrix.[22] With the incorporation of iron oxide, the degree of crystallinity and melting temperature (T_m) were slightly increased with respect to the values for the hydrogel, which can be attributed to an additional postcrystallization process occurring during a second drying step,[18] helped by the nucleating effect of the well-distributed NPs. This process would enable the formation of larger crystals with a higher melting temperature.

Table 1. Thermal Analysis of Hydro- and Ferrogel Samples[a]

	T_m (°C)	X_{cr} (%)	T_p (°C)	Fe_2O_3 (wt %)
hydrogel	220.5 ± 0.3	31.80 ± 3.2	284.3 ± 5.3	0
ferrogel	223.7 ± 0.6	35.3 ± 5.1	295.9 ± 6.4	15.7 ± 3.1

[a] T_m, melting temperature; X_{cr}, degree of crystallinity; T_p, degradation temperature; Fe_2O_3, iron oxide content.

It is important to note that, although the absolute value of crystallinity can be affected by the measurement method,[21,23] the values obtained here are similar to those found in the literature for PVA hydrogels obtained by F−T cycling.[24] Moreover, the increase in crystallinity observed in the case of the ferrogel was repeatedly observed independently of the method used for its measurement (XRD or DSC). This is important because it demonstrates that the presence of NPs does not interfere with the structure of the gel or its thermal properties.

Magnetic Properties. The mass magnetization (M) versus field (H) curves obtained for hydrated ferrogel samples are similar to those expected for an ensemble of noninteracting single-domain magnetic particles (see Figure 5 for the curves recorded for the hydrated ferrogel at temperatures between 10 and 290 K). At temperatures of 40 K and higher, no hysteresis was observed. The analysis of the curves for 290 and 300 K with a log-normal distribution of Langevin functions indicates a distribution of NP magnetic sizes with a mean moment of about 1800 μ_B and a mean diameter of $D_M \approx 6.4$ nm (standard deviation $\sigma_D \approx 2$ nm). This value departs considerably from that determined by the TEM observations (about 46%). Dipolar interactions between NPs might be responsible for this departure, as it is shown next that they cannot be disregarded in the present case and it has been reported that significant error in the estimation of NP sizes by magnetic measurements occurs when these interactions are relevant.[25]

Field-cooling (FC) and zero-field-cooling (ZFC) M versus T curves measured for dry and hydrated ferrogel samples are shown in Figure 6. The curve shapes are again similar to those reported for noninteracting single-domain magnetic NPs.[26] However, different mean blocking temperatures of $T_B^d \approx 25$ K and $T_B^h \approx 17$ K were observed for the dry and hydrated ferrogel samples, respectively (Figure 6). Taking into account that hydration (W_∞, the equilibrium swelling degree in bidistilled water at room temperature) gives rise to a 200% growth in ferrogel volume, the different blocking temperatures might originate from the existence of dipolar interactions among NPs and their dependence on the mean NP separation, d. Assuming a uniform NP space distribution, d would be 44% larger in the hydrated ferrogel sample. Assuming Néel relaxation, the barrier energy for NP moment reversal in the presence of dipolar interactions can be expressed as $E_b = K_{eff}V + \varepsilon$, where K_{eff} is the

dx.doi.org/10.1021/ie402652j | Ind. Eng. Chem. Res. 2014, 53, 214−221

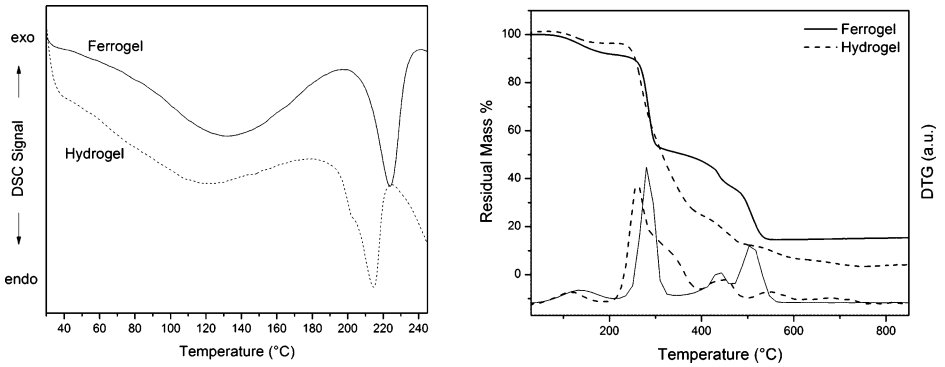

Figure 4. (a) DSC and (b) TGA and DTG curves for hydro- and ferrogels.

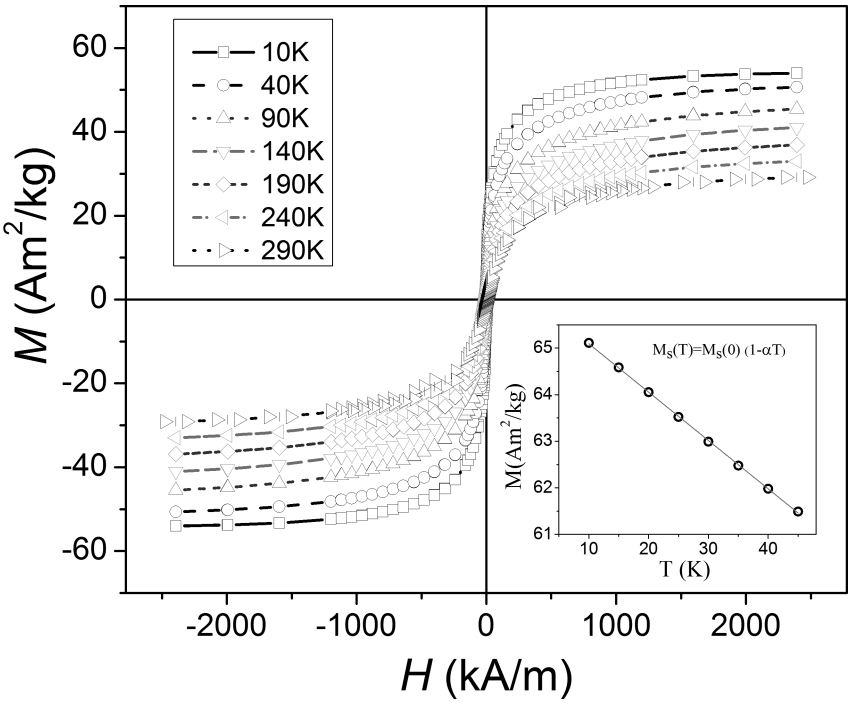

Figure 5. SQUID M vs H cycles obtained from the hydrated ferrogel sample at several temperatures from 10 to 290 K. Inset: Plot of saturation magnetization (M_S) vs T.

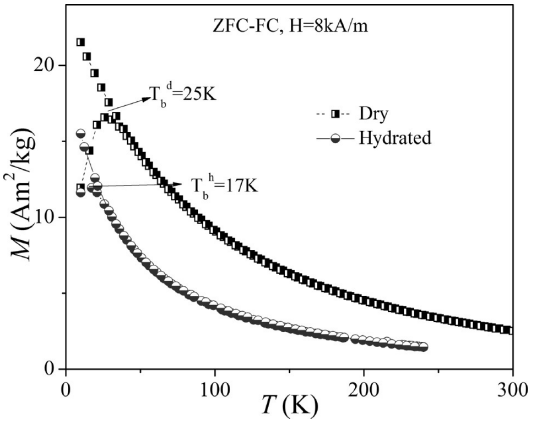

Figure 6. ZFC curve performed under a field of 7.96×10^3 A/m showing the temperature dependence of the magnetic moments of the hydrated and dry ferrogel samples. The NP mean blocking temperatures are 17 and 25 K, respectively.

NP effective anisotropy, V is the NP mean volume, and ε is the mean dipolar energy per NP.[26] Within this scenario, ε must be larger for the dry than hydrated ferrogel sample ($\varepsilon_d > \varepsilon_h$). From the proportionality between T_B and E_b,[26] a similar relationship must be expected for the corresponding blocking temperatures, that is, $T_B^d > T_B^h$ in accordance with experiments.

M versus H measurements at temperatures between 10 and 290 K also reveal the existence of NP interactions and suggest that the NP size obtained from magnetic measurements must be discussed in greater detail. Although M versus H curves can be well fitted using Langevin functions with arguments proportional to VM_SH/T with a log-normal NP size distribution, the results reveal strong hints of dipolar interactions, namely, a nonphysical but noticeable steady growth of the NP magnetic moment with temperature. The appearance of such behavior in data obtained from materials in which dipolar interactions between NPs cannot be disregarded is discussed by Allia et al. [25] A detailed account of the magnetic response of dry and hydrated materials presented in this article,

dx.doi.org/10.1021/ie402652j | Ind. Eng. Chem. Res. 2014, 53, 214−221

including the effect and quantification of dipolar interactions, will be presented in a future publication.

Swelling of Ferrogels. As observed in Figure 7, for varying immersion times, different volumes of iron salt solution were

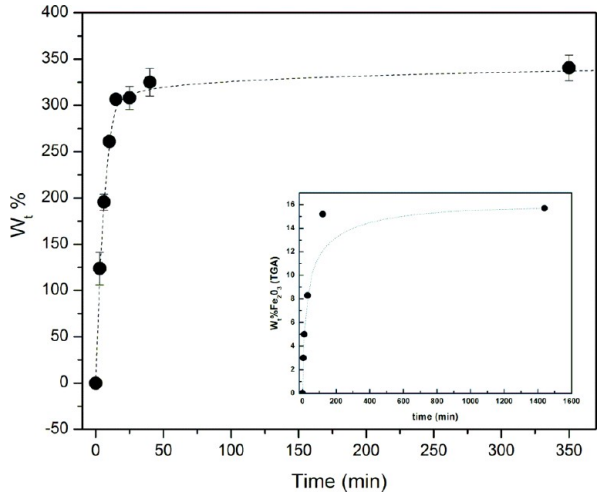

Figure 7. Hydrogel swelling as a function of time in an aqueous solution of iron salts. Inset: Iron oxide content (Fe_2O_3 weight percentage) as a function of time.

absorbed by the gel. As different amounts of solution contain different total amounts of iron oxide precursors, materials with different contents of NPs can be obtained by extracting samples at different immersion times. This can be observed for some selected samples in Figure 7 (inset), in which the total amount of iron oxide in the ferrogel measured by TGA is presented as a function of immersion time. It is important to note that the actual concentration of NPs in the final samples cannot be predicted accurately because of the possibility of a salt fractioning effect between the swollen gel and the outside solution (solution inside the gel could become more concentrated in salts than solution surrounding the gel because of the affinity of OH groups in PVA for cations). However, on a qualitative base, a higher loading of precursors, and consequently of NPs, can be expected for longer times of immersion in the precursor solution.

One of the main advantages of ferrogels obtained from PVA hydrogels cross-linked by F−T cycling can be found in their high swelling capacity in different solvents. The low cross-linking densities of these networks enable their use as efficient absorbers of a variety of biomolecules, drugs, and so on. As an example, Figure 8 shows the swelling behavior of ferrogels in ethanol solutions of ibuprofen [(*RS*)-2-(4-(2-methylpropyl)-phenyl)propanoic acid], a nonsteroidal anti-inflammatory drug of widespread use as an analgesic in common pharmacological treatments. As can be seen, replacing part of the water with ethanol produced a reduction in the solvent quality and in the equilibrium swelling value attained by the ferrogels (from 350% in water to about 100% in ethanol/water solutions). Despite this decrease in swelling capacity, the ferrogels still become considerably swollen in the presence of ethanol, which enables the loading of a drug with a poor solubility in water such as ibuprofen without precluding its ability for sustained release with time in aqueous environments at physiological pH (Figure 9).

It is known that drug concentration levels in blood plasma depend on the quantity of drug released from the used device.[27]

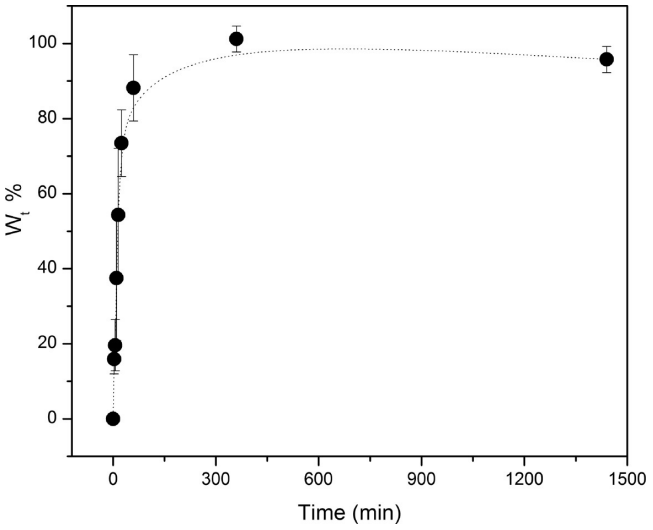

Figure 8. Swelling behavior of a ferrogel sample in an aqueous/ethanol ibuprofen solution.

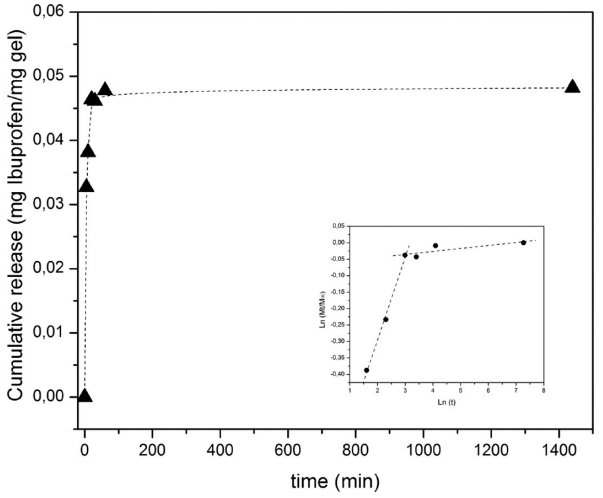

Figure 9. Release behavior of ibuprofen from a loaded ferrogel sample at physiological pH. Inset: $\ln(M_t/M_\infty)$ vs $\ln(t)$.

Hence, to evaluate the mobility of embedded molecules in hydrogels, these drug-delivery systems are usually characterized by release studies[28] In the simplest manner, the time-dependent swelling of a polymer has been generally described[29] by

$$M_t/M_\infty = kt^n \tag{3}$$

This equation is known as the power-law model, where n is the diffusional exponent. In this equation, M_t/M_∞ represents the fractional uptake of solvent (or release of a solute) normalized with respect to the equilibrium conditions. The variables k and n are constants that can be related to diffusion coefficients and the specific transport mechanism. This equation is used to account for the coupled effects of Fickian diffusion and viscoelastic relaxation in polymer systems[30]

As can be seen in Figure 9, the release of ibuprofen from the ferrogel in a buffer solution shows a high initial release rate followed by a low release rate (most of the drug was released in less than 150 min). Similar curves were obtained by Zhou et al.[14] and attributed to an initial rapid diffusion of drugs that mainly happened in the outermost layer of the sample. In the second stage of release, plots of $\ln(M_t/M_\infty)$ versus $\ln t$ showed

dx.doi.org/10.1021/ie402652j | Ind. Eng. Chem. Res. 2014, 53, 214−221

a linear behavior, suggesting that the drug-release process is in agreement with a diffusion-controlled mechanism (inset in Figure 9).

CONCLUSIONS

Ferrogels with well-dispersed single-domain magnetic NPs were obtained by a simple method based on the infusion of iron oxide precursors in a physical cross-linked PVA hydrogel, followed by coprecipitation of NPs in a basic medium. The thermal and magnetic properties of the materials were consistent with the formation of a homogeneous distribution of small iron oxide NPs in the matrix. The ability of the ferrogel to swell in different solvents allowed the absorption and subsequent release of ibuprofen, a drug with a low solubility in water, at physiological pH. The biocompatibility of the components, the magnetic and swelling behavior of the final materials, and the use of a nontoxic PVA cross-linking strategy (F−T cycling) make these materials promising for drug-delivery applications.

AUTHOR INFORMATION

Corresponding Author

*E-mail: jimena.gonzalez@fi.mdp.edu.ar. Tel.: +54 223 481 6600 ext 321.

Notes

The authors declare no competing financial interest.

ACKNOWLEDGMENTS

The authors sincerely thank National Research Council (CONICET), University of Mar del Plata (UNMdP), The National Agency for the Promotion of Science and Technology of Argentina (ANPCyT), and University of La Plata (UNLP) for financial support.

REFERENCES

(1) (a) Du, Y.; Shen, S. Z.; Cai, K.; Casey, P. S. Research progress on polymer−inorganic thermoelectric nanocomposite materials. *Prog. Polym. Sci.* **2012**, *37* (6), 820−841. (b) Nguyen, T.-P. Polymer-based nanocomposites for organic optoelectronic devices. A review. *Surf. Coat. Technol.* **2011**, *206* (4), 742−752. (c) Wang, Q.; Zhu, L. Polymer nanocomposites for electrical energy storage. *J. Polym. Sci. B: Polym. Phys.* **2011**, *49* (20), 1421−1429. (d) Sahoo, N. G.; Rana, S.; Cho, J. W.; Li, L.; Chan, S. H. Polymer nanocomposites based on functionalized carbon nanotubes. *Prog. Polym. Sci.* **2010**, *35* (7), 837−867. (e) Zhang, H.; Han, J.; Yang, B. Structural Fabrication and Functional Modulation of Nanoparticle−Polymer Composites. *Adv. Funct. Mater.* **2010**, *20* (10), 1533−1550. (f) Minelli, C.; Lowe, S. B.; Stevens, M. M. Engineering Nanocomposite Materials for Cancer Therapy. *Small* **2010**, *6* (21), 2336−2357. (g) Rozenberg, B. A.; Tenne, R. Polymer-assisted fabrication of nanoparticles and nanocomposites. *Prog. Polym. Sci.* **2008**, *33* (1), 40−112. (h) Paul, D. R.; Robeson, L. M. Polymer nanotechnology: Nanocomposites. *Polymer* **2008**, *49* (15), 3187−3204. (i) Vaia, R. A.; Maguire, J. F. Polymer Nanocomposites with Prescribed Morphology: Going beyond Nanoparticle-Filled Polymers. *Chem. Mater.* **2007**, *19* (11), 2736−2751. (j) Balazs, A. C.; Emrick, T.; Russell, T. P. Nanoparticle Polymer Composites: Where Two Small Worlds Meet. *Science* **2006**, *314* (5802), 1107−1110.

(2) (a) Aimé, C.; Coradin, T. Nanocomposites from biopolymer hydrogels: Blueprints for white biotechnology and green materials chemistry. *J. Polym. Sci. B: Polym. Phys.* **2012**, *50* (10), 669−680. (b) Fernández-Barbero, A.; Suárez, I. J.; Sierra-Martín, B.; Fernández-Nieves, A.; de las Nieves, F. J.; Marquez, M.; Rubio-Retama, J.; López-Cabarcos, E. Gels and microgels for nanotechnological applications. *Adv. Colloid Interface Sci.* **2009**, *147−148* (0), 88−108. (c) Schexnailder, P.; Schmidt, G. Nanocomposite polymer hydrogels. *Colloid Polym. Sci.* **2009**, *287* (1), 1−11. (d) Ko, D. Y.; Shinde, U. P.; Yeon, B.; Jeong, B. Recent progress of in situ formed gels for biomedical applications. *Prog. Polym. Sci.* **2013**, *38* (3−4), 672−701.

(3) Peppas, N. A.; Hilt, J. Z.; Khademhosseini, A.; Langer, R. Hydrogels in Biology and Medicine: From Molecular Principles to Bionanotechnology. *Adv. Mater.* **2006**, *18* (11), 1345−1360.

(4) (a) Seliktar, D. Designing Cell-Compatible Hydrogels for Biomedical Applications. *Science* **2012**, *336* (6085), 1124−1128. (b) Buenger, D.; Topuz, F.; Groll, J. Hydrogels in sensing applications. *Prog. Polym. Sci.* **2012**, *37* (12), 1678−1719. (c) Hoffman, A. S. Hydrogels for biomedical applications. *Adv. Drug Delivery Rev.* **2002**, *54* (1), 3−12. (d) Burdick, J. A.; Murphy, W. L. Moving from static to dynamic complexity in hydrogel design. *Nat. Commun.* **2012**, *3*, 1269.

(5) (a) Gonzalez, J. S.; Hoppe, C. E.; Alvarez, V. A. Poly (Vinyl Alcohol) Ferrogels: Synthesis and Applications. In *Advances in Materials Science Research*; Wythers, M. C., Ed.; Nova Science Publishers: New York, 2012; Vol. *13*. (b) Zrínyi, M. Colloidal particles that make smart polymer composites deform and rotate. *Colloids Surf. A* **2011**, *382* (1−3), 192−197. (c) Filipcsei, G.; Csetneki, I.; Szilágyi, A.; Zrínyi, M. Magnetic Field-Responsive Smart Polymer Composites. *Adv. Polym. Sci.* **2007**, *206*, 137−189.

(6) Liu, T. Y.; Hu, S. H.; Liu, D. M.; Chen, S. Y. Magnetic-sensitive behavior of intelligent ferrogels for controlled release of drug. *Langmuir* **2006**, *22* (14), 5974−5978.

(7) (a) Kumar, C. S. S. R.; Mohammad, F. Magnetic nanomaterials for hyperthermia-based therapy and controlled drug delivery. *Adv. Drug Delivery Rev.* **2011**, *63* (9), 789−808. (b) Knecht, L. D.; Ali, N.; Wei, Y.; Hilt, J. Z.; Daunert, S. Nanoparticle-Mediated Remote Control of Enzymatic Activity. *ACS Nano* **2012**, *6* (10), 9079−9086.

(8) Hu, S. H.; Liu, T. Y.; Liu, D. M.; Chen, S. Y. Controlled pulsatile drug release from a ferrogel by a high-frequency magnetic field. *Macromolecules* **2007**, *40* (19), 6786−6788.

(9) Moscoso-Londoño, O.; Gonzalez, J. S.; Muraca, D.; Hoppe, C. E.; Alvarez, V. A.; López-Quintela, A.; Socolovsky, L. M.; Pirota, K. R. Structural and magnetic behavior of ferrogels obtained by freezing thawing of polyvinyl alcohol/poly(acrylic acid) (PAA)-coated iron oxide nanoparticles. *Eur. Polym. J.* **2013**, *49* (2), 279−289.

(10) Hassan, C.; Peppas, N. Structure and Applications of Poly(vinyl alcohol) Hydrogels Produced by Conventional Crosslinking or by Freezing/Thawing Methods. *Adv. Polym. Sci.* **2000**, *153*, 37−65.

(11) Alves, M.-H.; Jensen, B. E. B.; Smith, A. A. A.; Zelikin, A. N. Poly(Vinyl Alcohol) Physical Hydrogels: New Vista on a Long Serving Biomaterial. *Macromol. Biosci.* **2011**, *11* (10), 1293−1313.

(12) Reséndiz-Hernández, P. J.; Rodríguez-Fernández, O. S.; García-Cerda, L. A. Synthesis of poly(vinyl alcohol)−magnetite ferrogel obtained by freezing−thawing technique. *J. Magn. Magn. Mater.* **2008**, *320* (14), e373−e376.

(13) (a) Gonzalez, J.; Hoppe, C.; Muraca, D.; Sánchez, F.; Alvarez, V. Synthesis and characterization of PVA ferrogels obtained through a one-pot freezing−thawing procedure. *Colloid Polym. Sci.* **2011**, *289* (17−18), 1839−1846. (b) Mendoza Zélis, P.; Muraca, D.; Gonzalez, J. S.; Pasquevich, G. A.; Alvarez, V. A.; Pirota, K. R.; Sánchez, F. H. Magnetic properties study of iron-oxide nanoparticles/PVA ferrogels with potential biomedical applications. *J. Nanopart. Res.* **2013**, *15* (5), 1−12.

(14) Zhou, L.; He, B.; Zhang, F. Facile One-Pot Synthesis of Iron Oxide Nanoparticles Cross-linked Magnetic Poly(vinyl alcohol) Gel Beads for Drug Delivery. *ACS Appl. Mater. Interfaces* **2011**, *4* (1), 192−199.

(15) (a) Feldgitscher, C.; Peterlik, H.; Puchberger, M.; Kickelbick, G. Structural Investigations on Hybrid Polymers Suitable as a Nanoparticle Precipitation Environment. *Chem. Mater.* **2009**, *21* (4), 695−705. (b) Reddy, N. N.; Varaprasad, K.; Ravindra, S.; Reddy, G. V. S.; Reddy, K. M. S.; Mohan Reddy, K. M.; Raju, K. M. Evaluation of blood compatibility and drug release studies of gelatin based magnetic hydrogel nanocomposites. *Colloids Surf. A* **2011**, *385* (1−3), 20−27. (c) Hernández, R.; Mijangos, C. In Situ Synthesis of Magnetic Iron Oxide Nanoparticles in Thermally Responsive Alginate-Poly(*N*-

isopropylacrylamide) Semi-Interpenetrating Polymer Networks. *Macromol. Rapid Commun.* **2009**, *30* (3), 176−181. (d) Caykara, T.; Yörük, D.; Demirci, S. Preparation and characterization of poly(*N*-*tert*-butylacrylamide-co-acrylamide) ferrogel. *J. Appl. Polym. Sci.* **2009**, *112* (2), 800−804.
(16) Ledo-Suárez, A.; Puig, J.; Zucchi, I. A.; Hoppe, C. E.; Gómez, M. L.; Zysler, R.; Ramos, C.; Marchi, M. C.; Bilmes, S. A.; Lazzari, M.; López-Quintela, M. A.; Williams, R. J. J. Functional nanocomposites based on the infusion or in situ generation of nanoparticles into amphiphilic epoxy gels. *J. Mater. Chem.* **2010**, *20* (45), 10135−10145.
(17) Willcox, P. J.; Howie, D. W., Jr.; Schmidt-Rohr, K.; Hoagland, D. A.; Gido, S. P.; Pudjijanto, S.; Kleiner, L. W.; Venkatraman, S. Microstructure of poly(vinyl alcohol) hydrogels produced by freeze/thaw cycling. *J. Polym. Sci. B: Polym. Phys.* **1999**, *37* (24), 3438−3454.
(18) Gonzalez, J. S.; Alvarez, V. A. The effect of the annealing on the poly(vinyl alcohol) obtained by freezing−thawing. *Thermochim. Acta* **2011**, *521* (1−2), 184−190.
(19) Peppas, N. A.; Merrill, E. W. Differential scanning calorimetry of crystallized PVA hydrogels. *J. Appl. Polym. Sci.* **1976**, *20* (6), 1457−1465.
(20) Iervolino, M.; Raghavan, S. L.; Hadgraft, J. Membrane penetration enhancement of ibuprofen using supersaturation. *Int. J. Pharm.* **2000**, *198* (2), 229−238.
(21) Ricciardi, R.; Auriemma, F.; Gaillet, C.; De Rosa, C.; Lauprêtre, F. Investigation of the crystallinity of freeze/thaw poly(vinyl alcohol) hydrogels by different techniques. *Macromolecules* **2004**, *37* (25), 9510−9516.
(22) Goiti, E.; Salinas, M. M.; Arias, G.; Puglia, D.; Kenny, J. M.; Mijangos, C. Effect of magnetic nanoparticles on the thermal properties of some hydrogels. *Polym. Degrad. Stab.* **2007**, *92* (12), 2198−2205.
(23) Hernandez, R.; Lopez, D.; Mijangos, C.; Guenet, J. M. A reappraisal of the 'thermoreversible' gelation of aqueous poly(vinyl alcohol) solutions through freezing−thawing cycles. *Polymer* **2002**, *43* (21), 5661−5663.
(24) (a) Hickey, A. S.; Peppas, N. A. Mesh size and diffusive characteristics of semicrystalline poly(vinyl alcohol) membranes prepared by freezing/thawing techniques. *J. Membr. Sci.* **1995**, *107* (3), 229−237. (b) Mongia, N. K.; Anseth, K. S.; Peppas, N. A. Mucoadhesive poly(vinyl alcohol) hydrogels produced by freezing/thawing processes: Applications in the development of wound healing systems. *J. Biomater. Sci., Polym. Ed.* **1996**, *7* (12), 1055−1064.
(25) Allia, P.; Coisson, M.; Tiberto, P.; Vinai, F.; Knobel, M.; Novak, M. A.; Nunes, W. C. Granular Cu−Co alloys as interacting superparamagnets. *Phys. Rev. B* **2001**, *64* (14), 144420.
(26) Dormann, J. L.; Fiorani, D.; Tronc, E. Magnetic Relaxation in Fine-Particle Systems. *Adv. Chem. Phys.* **2007**, *98*, 283−494.
(27) Bajpai, A.; Shukla, S. K.; Bhanu, S.; Kankane, S. Responsive polymers in controlled drug delivery. *Prog. Polym. Sci.* **2008**, *33* (11), 1088−1118.
(28) Brandl, F.; Kastner, F.; Gschwind, R. M.; Blunk, T.; Teßmar, J.; Göpferich, A. Hydrogel-based drug delivery systems: Comparison of drug diffusivity and release kinetics. *J. Controlled Release* **2010**, *142* (2), 221−228.
(29) Ritger, P. L.; Peppas, N. A. A simple equation for description of solute release I. Fickian and non-Fickian release from non-swellable devices in the form of slabs, spheres, cylinders or discs. *J. Controlled Release* **1987**, *5* (1), 23−36.
(30) Brazel, C. S.; Peppas, N. A. Modeling of drug release from swellable polymers. *Eur. J. Pharm. Biopharm.* **2000**, *49* (1), 47−58.